# FORECAST AND PREVISIBILITY OF BALLOON TRAJECTORIES IN THE LOW TROPOSPHERE

**C. Basdevant, E. Tromeur, and J.P. Duvel**

CNRS - Laboratoire de Météorologie Dynamique

École Normale Supérieure, 24 Rue Lhomond, 75231 Paris, FRANCE
*basdevant@lmd.ens.fr, tromeur@lmd.ens.fr, jpduvel@lmd.ens.fr*

## ABSTRACT

In the framework of the VASCO/CIRENE project, designed to investigate the ocean-atmosphere variability in the Indian Ocean from intra-seasonal to inter-annual times-scales, instrumented balloons are launched in the atmospheric boundary layer. Two types of balloons are used : small pressurized balloons designed to fly at a constant density level around 850hPa and Aéroclippers, a new aerostatic/buoying system that drifts approximately at an altitude of 50 meters.
To forecast the trajectories of these vehicles and optimize their launching strategy, an original software has been developed. This software uses the ten-day forecasts produced twice a day by the European Centre for Medium-range Weather Forecasts (ECMWF). To evaluate the confidence of numerical trajectories and their previsibility, two strategies are implemented. The first one detects mostly the spatio-temporal phase errors in the meteorological forecast, while the second one detects the variability due to the uncertainty on the forecast initial state.

Key words: Balloon;Trajectory;Forecasts;ECMWF.

## 1. INTRODUCTION

The deep convective activity over the Indo-Pacific region is strongly modulated at time scales between 20 and 60 days. This intraseasonal variability has a marked seasonal cycle with an eastward propagation of the convective perturbations, close to the equator, from the Indian to the western Pacific Oceans, during the boreal winter. This phenomenon is generally referred to as the Madden-Julian oscillation (12) and may interact with the El Niño-Southern Oscillation (ENSO) (11; 14). During the boreal summer, the eastward propagation along the equator over the Indian Ocean is followed by a northward propagation of the convective perturbations from the equator into the Indian peninsula (10). These intraseasonal perturbations have an impact on the Indian monsoon (3) and may even influence its seasonal mean and its interannual variability (13; 6).
To investigate the ocean-atmosphere variability in the Indian Ocean, from intra-seasonal to inter-annual times-scales, the VASCO/CIRENE project is conducted jointly by the Laboratoire de Météorologie Dynamique (LMD) and the French Space Agency (CNES). In the framework of this experiment, two types of instrumented balloons are launched, from Mahé (Seychelles), in the atmospheric boundary layer. First of all, small pressurized balloons, designed to fly at a constant density level around 850hPa, allow us to probe the upper part of the boundary layer. Then a new aerostatic/buoying system, named Aéroclipper, designed to investigate the atmosphere ocean fluxes, is based on a tetrahedral balloon, pulled by the wind at an altitude of approximately 50 meters, attached by a cable (the guiderope) to a oceanic measurement gondola floating just under the sea surface.

The first objective of the research project reported here was to develop a set of operational tools, based on meteorological forecasts, for the assistance to the launching decisions of these aerostats during the field campaign. Beyond, the second objective was, after the probatory experiment, to analyze discrepancies between actual and simulated trajectories.
The optimization of the launching strategy during the VASCO experiment is mandatory since, due to their cost, the number of balloons is limited and we want them to explore at best the region of interest. Moreover balloons ought to fly over the ocean and avoid inhabited regions for security reasons. Numerical trajectories, computed from operational meteorological forecasts, have been the base of our operational forecasting system. This software uses the

ten-day meteorological forecasts produced twice a day by the ECMWF. Numerically, pressurized balloons are advected on isopycnic (constant density) surfaces while Aéroclippers are moved using a dedicated non-linear function of the 10-meter level wind. This non-linear function has been experimentally determined to take into account the drag induced by the guiderope and the oceanic gondola.
In order to evaluate the confidence of these numerical trajectories and their predicability, two strategies have been developed. The first strategy is based on the full resolution deterministic ECMWF forecasts. We follow the dispersion of an initial set of 50 balloons launched on a 50km radius circle around Mahé. The second strategy uses the probabilistic ECMWF forecasts: 50 lower-resolution perturbed forecasts and one control forecast, supplied by the ECMWF, allow us to compute 51 possible trajectories for one balloon launched at Mahé. These two methods, automatically brought into play in parallel twice a day, provide informations about the possible behaviour of a real balloon. The first one detects mostly the spatio-temporal phase errors in the meteorological forecast, while the second detects the variability due to the uncertainty on the forecast initial state.

The balloon characteristics will be summarized in section 2; in section 3 we present the main lines of our software before comparing, in section 4, the forecast trajectories to the actual ones obtained during the probatory VASCO experiment that took place in February 2005. A general conclusion is presented in section 5.

## 2. BALLOONS CHARACTERISTICS

### 2.1. Small pressurized balloons

Fruits of a cooperation between CNES, and LMD, small pressurized balloons (SPB) have been already used to study the boundary layer dynamics during BALSAMINE, INDOEX and BOA experiments (2; 5; 4). Superpressure balloons keep a nearly constant volume and therefore fly at a quasi-constant density level, acting as Lagrangian tracers of air parcels and meteorological platforms. VASCO balloons, produced by ZODIAC under CNES supervision, are inflated with helium with a nominal 120hPa overpressure at flight level. The envelope, made of three-laminated polyester of 125$\mu$m, has a 2.5m diameter spherical shape (Figure 1). With a total mass of approximately 9kg, this vehicle can fly in layers between the surface and approximately 830hPa depending of its ballast. As long as a sufficient overpressure is maintained the volume remains constant, except for slight thermal fluctuations producing low amplitude buoyancy oscillations mostly driven by the diurnal cycle.

*Figure 1. Launching of a SPB on Mahé airport.*

The dynamics of superpressure balloons has been studied by several authors (1; 7; 9). They proved to be good tracers of horizontal motion close to their equilibrium density level. However, they may react to wind bursts by small amplitude, high frequency, vertical oscillations around this equilibrium level. The most serious problem they encounter is water loading by rain or condensation when the envelope temperature drops under the dew point temperature. This latter case may happen when the balloon enters nearly saturated air or whenever the helium gets cooled by nocturnal radiation.
Scientific instrumentation on board SPB's consists in air pressure, temperature and humidity sensors, and a 3D location GPS receiver. Helium temperature and pressure are also recorded. Data are broadcasted, with a mean 15 minutes period, through the ARGOS system. Power is provided by lithium batteries that ensure around a one month lifetime. Batteries, electronics, ARGOS and GPS antenna are all located inside the envelope, protected from salty water when the balloon hits or gets close to the sea surface.
Five balloons and their payload were prepared, tested and launched with success from Mahé island (Seychelles) during February 2005 for the VASCO probatory campaign.

### 2.2. Aéroclippers

Developed jointly by LMD, LOCEAN, ENSTA and CNES, the Aéroclipper is a new aerostatic/buoying system based on a balloon attached by a 80m long guiderope to a gondola floating just below the sea surface (Figure 2). The balloon has a tetrahedral shape, with a 6m edge, and drifts at an altitude of approximately 50m. The technical and scientific payloads are distributed in four gondolas. Three of them are disposed along the guiderope in the atmospheric layer, the third one is the oceanic gondola. Below the balloon the first gondola (NSO), devoted to security control, includes a 3D GPS receiver and an ARGOS

*Figure 2. The Aéroclipper in flight.*

transmitter. The second gondola, 15m below the balloon, is the atmospheric one. It records air temperature, pressure and humidity and also horizontal relative wind with a sonic anemometer. The third gondola (NTS), hosts a 2D GPS receiver and ensures data treatment and broadcasting through the ARGOS system with a period that may vary between 1 and 15 minutes. At last, the oceanic gondola includes a lochmeter, a thermo-salinometer and two thermometers recording the water temperature at 10 and 40cm below the sea surface. Lithium batteries ensure a one month autonomy for this system. The instrumentation is designed to estimate the turbulent momentum, heat and humidity fluxes at the ocean atmosphere interface.
Four Aéroclippers have been launched with success during the 2005 probatory VASCO campaign.

## 3. TRAJECTORY FORECAST MODEL

### 3.1. Numerical scheme

The computation of forecast trajectories proceeds in a similar way for SPB's and Aéroclippers, except that SPB's request for a vertical interpolation to the proper density level, while Aéroclippers only use the 10-meter level wind. The basic principle of the numerical model for balloon advection is that, given the horizontal wind fields produced operationally by the ECMWF for the next ten days, this wind is interpolated in time and space at the balloon location and then the balloon can be advected using a second order Runge-Kutta scheme with a 20mn time step (it is well known that the order two accuracy is greatly sufficient compared to the uncertainty in the wind field, see e.g. (8)). For the time interpolation of ECMWF data we use a knot-a-knot cubic spline interpolation on three values on each side of the time of interest, and for horizontal interpolation a knot-a-knot cubic spline interpolation on four points on each side of the point of interest in each direction. We already noted that the Aéroclipper advection velocity is deduced from the 10-meter level wind produced by ECMWF through a dedicated non-linear function. As our model also includes a land-sea mask, an Aéroclipper is numerically stopped if it happens to reach a coast. For SPB's we use the ECMWF wind fields on 20 original hybrid horizontal levels ranging from the surface up to roughly 500hPa; the vertical interpolation to the desired density level is then done by means of a knot-a-knot cubic spline interpolation in the density logarithm on all these 20 levels. As the lowest hybrid level follows the topography, a crash of a SPB can be detected (an event most unlikely during the VASCO experiment).

### 3.2. Meteorological data

The ECMWF produces twice a day two types of forecasts: the deterministic (FC) and the probabilistic (PF) forecasts. Both types start from an initial state at time J (equal to 00h or 12hUTC) and last 10 days (until J+240h). The deterministic forecast uses a full resolution, spectral T511, 60 levels, model to compute one ten-day forecast; the data we used with this deterministic forecast are produced on a regular $0.5^o \times 0.5^o$ longitude×latitude grid. The probabilistic system uses a spectral T255, 40 levels, model to compute one ten-day control forecast and 50 ten-day perturbed forecasts, the perturbation being introduced randomly, in the initial state, on the most unstable components. The data we used from these 51 probabilistic forecasts are produced on a regular $1^o \times 1^o$ longitude×latitude grid; as wind fields are available only on standard pressure level for probabilistic forecasts, the SPB advection was done in that case on the 850hPa isobaric surface. Concerning the times at which the wind field are available, they are, for the deterministic forecast, every 3h from J to J+72h, then every 6h until J+240h; for the probabilistic forecasts they are every 6h from J to J+240h.

### 3.3. The operational forecasting system

A fully automatic computer system has been developed, able to recover routinely the ECMWF

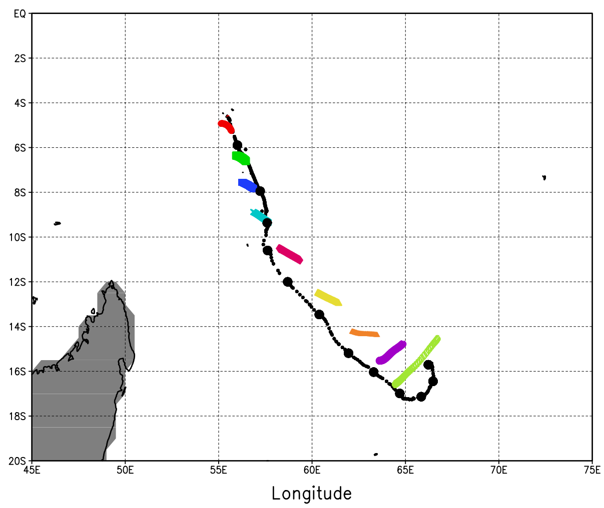


*Figure 3. Aéroclipper 3: actual trajectory (solid line with dotted positions at 12UTC) and deterministic forecast (positions of the 50 numerical Aéroclippers at 12UTC).*

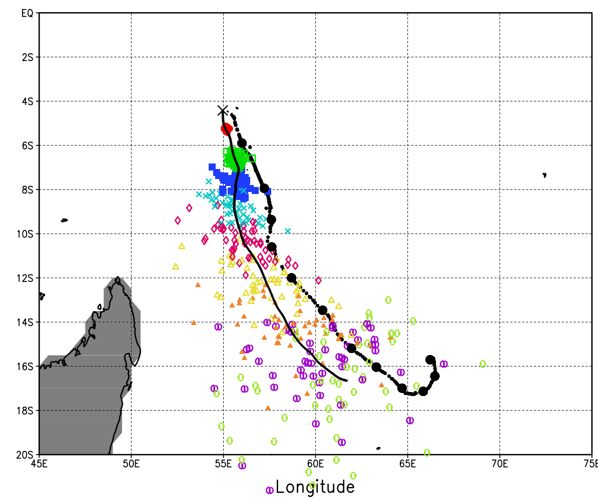


*Figure 4. Aéroclipper 3: actual trajectory (as in Figure 3) and daily 12UTC positions of probabilistic forecasts (the control forecast is in thin solid line).*

forecasts, as soon as they are available, to compute balloons trajectories and auxiliary meteorological maps and to post them on the web (http://www.lmd.ens.fr/vasco2005/) at the disposal of the launching team in Mahé.
For each available ECMWF forecast 15 sets of balloons and 15 sets of Aéroclippers are numerically launched, every 6 hours, at launching times from J+12h to J+96h (J+4 days). With the deterministic forecasts each set consists in 50 aerostats distributed on a 50km radius circle around Mahé, while for each 51 probabilistic forecast only one balloon is launched from Mahé island. For the SPB's and the deterministic forecasts three density levels have been selected on which 15×50 balloons are advected, these densities are: 1.00 kg/m$^3$ ($\approx$ 830hPa), 1.05 kg/m$^3$ ($\approx$ 880hPa), 1.10 kg/m$^3$ ($\approx$ 930hPa). Secondarily the operational system displays comparisons of trajectory forecasts corresponding to the same launching date but computed with different meteorological forecasts. These drawings allow us to evaluate the stability and the relevance of the predictions. In practice, all these results are available on the web at J+8h.

## 4. RESULTS AND DISCUSSION

The complete analysis of the VASCO 2005 probatory experiment is steel under way, however interesting insights have already been obtained by comparing the forecasted and actual trajectories. We will present first the Aéroclippers's behavior then the SPB's.

### 4.1. Aéroclipper's trajectories

The third Aéroclipper (A3) was launched from Mahé on February 24 at 03hUTC; if flew during 11 days, until March 7 at 12hUTC. The A3 trajectory is drawn on Figures 3 and 4 in solid line with larger dots at daily 12UTC positions. On Figure 3 are also drawn the daily positions at 12UTC of the 50 numerical Aéroclippers launched on a 50km radius circle around Mahé on February 24 at 00UTC. Their trajectories have been computed with the ECMWF deterministic forecast starting on February 23 at 12UTC (the most recent forecast available before launch time). Similarly, Figure 4 is a comparison of the A3 trajectory to its probabilistic forecasts, that is to the 51 trajectories computed with the 51 low resolution ECMWF forecast runs. The thin solid line corresponds to the low resolution control forecast (unperturbed initial state); the daily 12UTC positions of the 50, initially perturbed, forecasts are indicated with various symbols.
The first result that appears by comparing Figures 3 and 4 is the difference between the mean deterministic forecast (on Figure 3) and the control forecast on Figure 4: they separate quite rapidly, the latter being more southward. Moreover the deterministic forecast is much closer to the actual trajectory of A3. This highlights the resolution effect on forecasts: indeed the deterministic forecast is computed with a twice better resolution than the probabilistic ones.
The second result that is clearly seen on Figures 3 and 4 is the very different dispersion properties of deterministic and probabilistic forecasts. The initial circle of balloons in the deterministic forecast has a size of the order, though larger, than the model resolution. It deforms slowly under the effects of small scale shears. Initially shrunk in the North-South di-

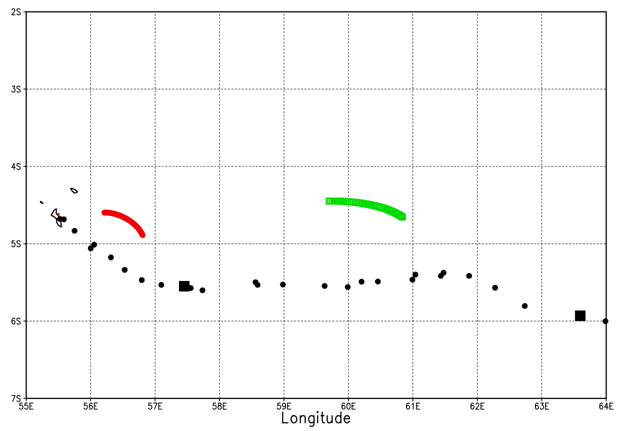


*Figure 5. Balloon 2: actual trajectory and deterministic forecast for the first 1.5 days of flight. Dark squares indicate the position of SPB 2 on, respectively, February 17, 00hUTC and 18, 00hUTC. Numerical balloons positions are drawn for the same times.*

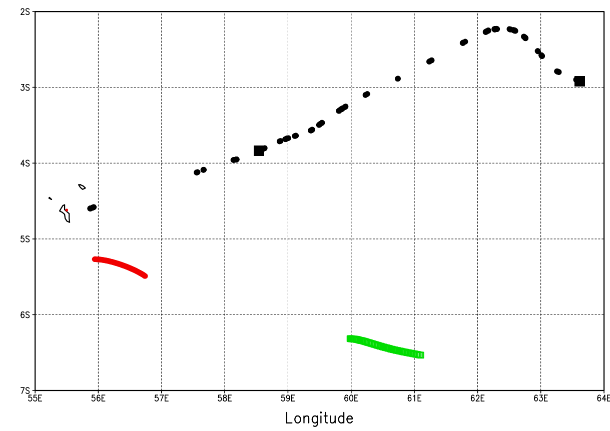


*Figure 6. Balloon 3: actual trajectory and deterministic forecast for the first 1.5 days of flight. Dark squares indicate the position of SPB 3 on, respectively, February 20, 00hUTC and 21, 00hUTC. Numerical balloons positions are drawn for the same times.*

rection, it is gradually extended in the East-West one. Starting at a size of 50km, it attains, 9 days later, nearly 300km. On the other side, the effect of the uncertainty on the initial state, as included in ECMWF probabilistic forecasts, is much larger and appears to disperse strongly the balloons in the longitudinal direction, the A3 trajectory being at the eastern boundary of the probabilistic positions cloud. It appears thus on Figure 3 that the deterministic forecast is a good predictor of the Aéroclipper's trajectory for nearly one week, however when looking to its velocity along the trajectory, we find it underestimated in the simulation, at least for low values of the 10-meter wind. This is seen at the beginning of the flight: the numerical balloons are, after 2 days, almost one day backward the actual one. This behavior may indicate a deficiency of our non-linear modelization of the Aéroclipper velocity or alternatively an underestimation of the 10-meter wind by the ECMWF.

### 4.2. SPB's trajectories

The comparison between SPB's actual and forecasted trajectories is difficult because of the possible vertical excursions of the balloons. Indeed the actual SPB's are not strictly isopycnic while the numerical ones are. Real balloons may undergo slight vertical movements due to the daily thermo-dynamical cycle, also, as already mentioned, they may fall down quite deeply when encountering heavy showers or nocturnal condensation. Moreover for the preliminary campaign we report one, we do not have a full confidence on the pressure sensors in use. Thus our comparisons will be restricted to a limited initial part of the trajectories during which the SPB behavior can be considered as isopycnic with a good precision.

Figure 5 and 6 are devoted to the first 1.5 days of flight of respectively SPB 2 (launched on February 16, 12h32UTC) and SP3 (launched on February 19, 13h41UTC). Together with the actual positions are drawn the positions of the 50 numerical balloons of the deterministic forecast advected on the 1.00 kg/m$^3$ density surface on which both balloons were approximately flying. As for the Aéroclipper's case, the forecast in use was the most recent forecast available before launch time, the numerical launching time being 12UTC. On both examples large differences between experimental and numerical behaviors appear; the discrepancies develop both in displacement direction and in velocities. In both cases numerical balloons are advected much slower than actual ones.

SPB 4 had a 8.7 days flight that was almost isopycnic at density level 1.02 kg/m$^3$ and isobaric at pressure level 860hPa. It moved quite rapidly during 4 days (Figure 7), then remains sticked around 60.5 East, 10 South until it disappeared (probably due to a failure of the broadcasting system). On Figure 7 are also drawn the balloon positions in the corresponding probabilistic, 9 days, 850hPa level, forecast (same drawing conventions than for Aéroclippers). This last figure point out the limit of this forecasting procedure of SPB's behavior, this limit itself denounces a probable defect of ECMWF forecasted wind fields in the boundary layer.

## 5. CONCLUSION

We have setup an operational automatic and powerful system to forecast the trajectories of Aéroclippers and Small Pressurized Balloons in the boundary

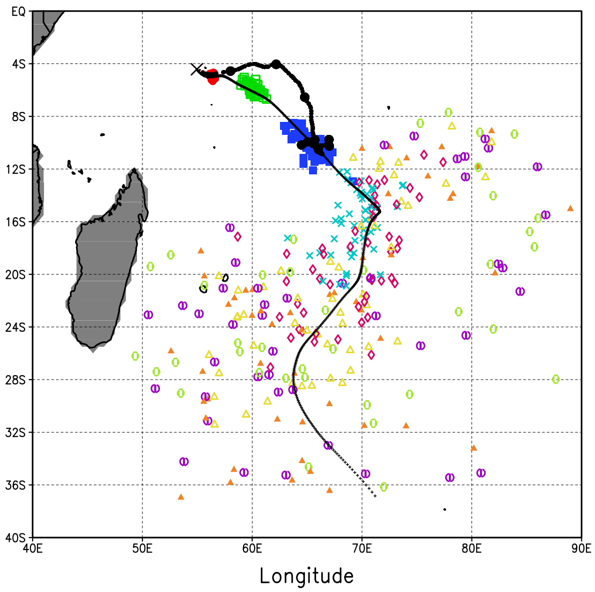


*Figure 7. Balloon 4: actual trajectory and probabilistic forecast. Large dots, for SPB 4, and symbols, for numerical balloons, indicate the positions every other day at 00hUTC.*

layer. This system is based on the deterministic and probabilistic meteorological forecasts produced by the ECMWF. This system was invaluable for launching operations during the probatory VASCO experiment that took place in Mahé (Seychelles) in February 2005 and will be used during the main VASCO campaign, planned for January 2006 and 2007. However the comparison between experimental and numerical trajectories exhibit significant differences, especially for SPB's. These differences, that we plan to examine in detail, may indicate systematic errors in wind fields produced in the boundary layer by the ECMWF.

## ACKNOWLEDGMENTS

This project was funded by the Centre National d'Études Spatiales (CNES) and the CNRS - Programme National d'Étude du Climat (PNEDC). The authors are indebted with the European Center for Medium-range Weather Forecasts who provided us daily real time forecasts and analysis. The authors thank the CNES and LMD balloon teams who developed the aerostats and operated them with imagination and efficiency.

## REFERENCES

[1] Colin J.L., Renard D., Lescoat V. *et al.*, Relationship between rain and snow acidity and air mass trajectory in eastern France, *Atmospheric Environement*, Vol. 23, 1487-1498, 1989.

[2] Cadet D.L., Ovarlez H. and Sommeria G., The BALSAMINE experiment, *Bull. Am. Meteo. Soc.*, 62, 381-388, 1981.

[3] Duvel J.P., Rocca R. and Vialard J., Ocean Mixed Layer Temperature Variations Induced by Intraseasonal Convective Perturbations over the Indian Ocean, *J. Atmos. Sci.*, Vol. 61, 1004-1023, 2004.

[4] Ethé C.H., Modélisation et Simulation de Trajectoires de Ballons Dérivants : Applications à l'Etude de la Circulation Atmosphériques sur l'Océan Indien, *Thèse de Doctorat de l'Université Paris XI*, 2001.

[5] Ethé C., Basdevant C., Sadourny R., Appru K.S., Harenduprakash L., Sarode P.R. and Viswanathan G., Air mass motion, temperature and humudity over the Arabian Sea and western Indian Ocean during the INDOEX intensive phase, as obtained from a set of superpressure drifting balloons, *J. Geophys. Res.*, Vol. 107, 8023, doi:10.1029/2001JD001120, 2002.

[6] Goswami B.N. and Mohan R.S.A., Intraseasonal oscillations and interannual variability of the Indian summer monsoon, *J. Climate*, Vol. 14, 1180-1198, 2001.

[7] Hanna S.R. and Hoecker W.H., The Response of Constant Density Balloons to Sinusoidal Variations of Vertical Wind Speeds, *Journal of Applied Meteorology*, Vol. 10, 601-604, 1971.

[8] Hertzog A., Basdevant C., Vial F. and Mechoso C.R, The accuracy of stratospheric analyses in the northern hemisphere inferred from long-duration balloon flights, *Q.J.R. Meteorol. Soc.*, 130, 607-626, 2004.

[9] Hirsh J.H. and Booker D.R., Response of Surpressure Balloons to Vertical Air Motions, *Journal of Applied Meteorology*, Vol. 5, 226-229, 1966.

[10] Lawrence D.M. and Webster P.J., The boreal summer intraseasonal oscillation : Relationship between northward and eastward movement of convection, *J. Atmos. Sci.*, Vol. 59, 1593-1606, 2002.

[11] McPhaden M.J., Genesis and evolution of the 1997-1998 El Niño, *Science*, Vol. 238, 950-954.

[12] Madden R.A. and Julian P.R., Observations of the 40-50 day tropical oscillation-A review, *Mon. Wea. Rev.*, Vol. 122, 814-836, 1994.

[13] Webster P.J., Magana V.O., Palmer T.N., Shukla J., Tomas R.A., Yanai M. and Yasunari T., Monsoons : Processes, predictability, and the prospects for prediction, *J. Geophys. Res.*, Vol. 103 (C7), 14451-14510, 1998.

[14] Zhang C., Hendon H.H., Kessler W.S. and Rosati A.J., A workshop on the MJO and ENSO, *Bull. Amer. Meteor. Soc.*, Vol. 82, 971-976, 2001.